



|                    |  |
|--------------------|--|
| <b>Title</b>       | <b>The Derived Equivalent Circuit Model for Magnetized Anisotropic Graphene</b>  |
| <b>Author(s)</b>   | <b>CAO, Y; Li, P; Jiang, L; Ruehli, ALBERT</b>   |
| <b>Citation</b>    | <b>IEEE Transactions on Antennas and Propagation, 2017, v. 65, p. 948-953</b>  |
| <b>Issued Date</b> | <b>2017</b>  |
| <b>URL</b>         | <b><a href="http://hdl.handle.net/10722/248407">http://hdl.handle.net/10722/248407</a></b>   |
| <b>Rights</b>      | <b>IEEE Transactions on Antennas and Propagation. Copyright © IEEE.; ©2017 IEEE. Personal use of this material is permitted. Permission from IEEE must be obtained for all other uses, in any current or future media, including reprinting/republishing this material for advertising or promotional purposes, creating new collective works, for resale or redistribution to servers or lists, or reuse of any copyrighted component of this work in other works.; This work is licensed under a Creative Commons Attribution-NonCommercial-NoDerivatives 4.0 International License.</b> |

# The Derived Equivalent Circuit Model for Magnetized Anisotropic Graphene

Ying S. Cao, *Student Member, IEEE*, Li Jun Jiang, *Senior Member, IEEE*, and Albert E. Ruehli, *Life Fellow, IEEE*

**Abstract**—Due to the static magnetic field, the conductivity for graphene becomes a dispersive and anisotropic tensor, which complicates most modeling methodologies. In this paper, a novel equivalent circuit model is proposed for graphene with the magnetostatic bias based on the electric field integral equation (EFIE). To characterize the anisotropic property of the biased graphene, the resistive part of the unit circuit is replaced by a resistor in series with current control voltage sources (CCVSs). The CCVSs account for the off-diagonal parts of the surface conductivity tensor for the magnetized graphene. Furthermore, the definitions of the absorption cross section ( $\sigma_{abs}$ ) and the scattering cross section ( $\sigma_{sca}$ ) are revisited to make them feasible for derived circuit analysis. This proposed method is benchmarked with several numerical examples. This paper also provides a new equivalent circuit model to deal with dispersive and anisotropic materials.

**Index Terms**—equivalent circuit, magnetized graphene, dispersive media, anisotropic conductivity

## I. INTRODUCTION

GRAPHENE, a two-dimensional version of graphite, is a very promising material in emerging nanoelectric devices, such as transistors [1], tunable terahertz (THz) antennas [2] and surface plasmon waveguides [3]. The surface conductivity of atomic-thick graphene denoted as  $\sigma_g(\omega, \mu_c, t, T)$  plays a pivotal role in the surface plasmon polariton (SPP), nano-patch antenna and so on.  $\sigma_g$  is a function of temperature  $T$ , chemical potential  $\mu_c$  (dependent on carrier density, electrostatic bias, chemical doping), and relaxation time  $t$ . By dynamically tuning the surface conductivity, the propagation, polarization, radiation and scattering properties of electromagnetic waves through graphene can be manipulated.

In order to model its gyrotropic effect, a two-dimensional graphene can be numerically characterized through the scalar conductivity [4] without the magnetic bias. Some numerical methods are emerging to deal with the scalar conductivity of graphene, such as, the method of moments (MOM) [5], finite difference time domain (FDTD) [6] method, and the partial element equivalent circuit (PEEC) method [7]. For FDTD method, it turns the surface conductivity of graphene into the complex permittivity by dividing the thickness of graphene. Afterwards, by applying three dimensional meshes, the finite difference method can solve this two-dimensional geometry clumsily. For the integral-based algorithms, for

example, the MOM method, it can directly implement the surface conductivity into the numerical process, but the physical process of how the magnetostatic field affects the properties of graphene is not clear since this is a pure mathematical process. Among these numerical methods, PEEC has its natural advantage over any other methods. It not only proposes an equivalent circuit model for graphene which can capture the physical characteristics, but also it applies the surface conductivity graphene directly without involving volumetric meshes, which significantly reduces the time consumption and memory size.

However, with the bias by a static magnetic field, the surface conductivity of graphene becomes an anisotropic tensor [8], [9], which complicates the problem. Hence, the numerical methods have to settle the dispersive and anisotropic properties of graphene simultaneously. In [10], a FDTD approach is developed by transforming the 2D Drude-model surface conductivity of graphene into a volumetric tensor, and implementing it by using the auxiliary differential equation (ADE) and the matrix exponential method. However, this method uses volumetric discretizations, which slows the computation.

In this paper, a novel circuit model based on the electric field integral equation (EFIE) is proposed to solve the dispersivity and anisotropy of magnetostatically biased graphene. In the equivalent circuit model, the diagonal elements of the surface conductivity tensor intrinsically correspond to the resistance of each inductive branch, which is the same as the unbiased scalar conductivity of graphene [4]. For the off-diagonal elements of the conductivity tensor, a new equivalent circuit model is developed to model the resistive characteristics by utilizing current control voltage sources (CCVSs). The CCVSs are in series with the intrinsic resistors. To demonstrate our proposed method, several numerical examples are compared with the results from other numerical methods. These CCVSs in the circuit quantitatively analyze how the magnetostatic field manipulates the electromagnetic characteristics of graphene. According to our best knowledge, no literature has ever developed the equivalent circuit modeling for dispersive and anisotropic graphene structures. Beyond graphene, this paper also extends PEEC method from handling isotropic materials to anisotropic and dispersive materials.

The remaining part of this paper is organized as follows: In Section II, the theory and formulations of the anisotropic conductivity tensor, and a brief introduction to the equivalent circuit method are addressed. In Section III, details of the new equivalent circuit method for anisotropic graphene are carefully demonstrated, including derivations of the  $x$ - and  $y$ -directional equivalent circuit model. Section IV investi-

Ying S. Cao and Li Jun Jiang are with the Department of Electrical and Electronic Engineering, The University of Hong Kong, Hong Kong (e-mail: caoying@eee.hku.hk; jianglj@hku.hk)

Albert E. Ruehli is with UMRI/MST EMC Laboratory, Missouri University of Science and Technology, Rolla, MO 65409, USA (e-mail: albert.ruehli@gmail.com)

gates several numerical examples to benchmark our proposed method. Conclusions are made at the end of this paper.

## II. THEORY AND FORMULATIONS

### A. The Surface Conductivity Tensor

A graphene patch is placed in air, and a plane wave is linearly polarized along the length of the patch, which is illustrated in Fig. 1.

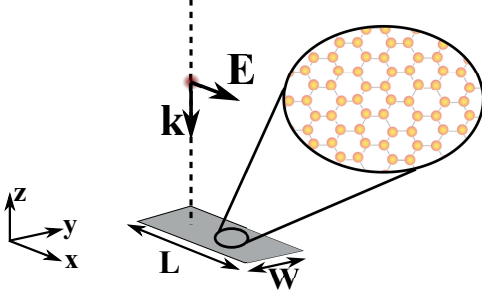


Fig. 1. Sketch of a graphene film placed in air, and a plane wave is linearly polarized along the length of the patch.  $L$  and  $W$  are the length and width of the graphene patch, respectively.

In the presence of the static magnetic field, the surface conductivity of graphene becomes a tensor  $\bar{\bar{\sigma}}_g$  [15], [17]. It satisfies  $\sigma_{xx} = \sigma_{yy} = \sigma_d$ ,  $-\sigma_{xy} = \sigma_{yx} = \sigma_o$ . Based on this fact, the conductivity of the magnetized graphene is written as

$$\bar{\bar{\sigma}}_g = \begin{pmatrix} \sigma_d & -\sigma_o & 0 \\ \sigma_o & \sigma_d & 0 \\ 0 & 0 & 0 \end{pmatrix} \quad (1)$$

According to the boundary condition on the graphene surface, we have

$$\hat{\mathbf{n}} \times (\mathbf{H}^+ - \mathbf{H}^-) = \mathbf{J}^{surf} = \bar{\bar{\sigma}}_g \mathbf{E} \quad (2)$$

where  $\mathbf{J}^{surf}$  is the surface current density on the graphene patch. The surface current density becomes

$$J_x^{surf} = \sigma_d E_x - \sigma_o E_y \quad (3a)$$

$$J_y^{surf} = \sigma_o E_x + \sigma_d E_y \quad (3b)$$

In preparation for the next section, we will graphically analyze the current density  $\mathbf{J}$  due to an electric field in the  $+x$ -direction, which is illustrated in Fig. 2. A  $y$ -directional current  $\mathbf{J}_y = \sigma_o \mathbf{E}_x$  is induced because of the off-diagonal term  $\sigma_o$  in the conductivity tensor.

The surface conductivity is composed of both intraband and interband contributions, which is further explained in the Appendix. Even though the intraband contribution dominates the surface conductivity in the THz frequency range, the proposed method in this paper can be applied using either rigorous or approximated formulations. In this paper, in order to improve the accuracy of the results, rigorous formulations of the conductivity (13) and (14) are applied throughout the paper.

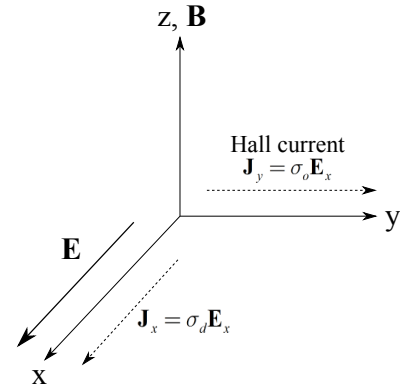


Fig. 2. Currents in  $x$  and  $y$  (according to Hall effect) directions according to electric field in  $+x$ -direction and anisotropic surface conductivity of graphene. The magnetic field is directed along the  $+z$ -axis.

### B. The Derived Circuit Based on EFIE

According to the electric field integral equation (EFIE), the total electric field is the superposition of incident field and the scattered field. Hence, we have

$$\mathbf{E}^{inc}(\mathbf{r}, \omega) = \frac{\mathbf{J}(\mathbf{r}, \omega)}{\sigma} + \mu \int_{v'} s G(\mathbf{r}, \mathbf{r}') \mathbf{J}(\mathbf{r}', \omega) dv' + \frac{\nabla}{\varepsilon} \int_{v'} G(\mathbf{r}, \mathbf{r}') q(\mathbf{r}', \omega) dv' \quad (4)$$

Here,  $s = j\omega$ , and  $G(\mathbf{r}, \mathbf{r}')$  is the full-wave Green's function. The partial inductance between cell  $\alpha$  and  $\beta$  and partial coefficient of potential between cell  $i$  and  $j$  can be represented as

$$Lp_{\alpha\beta} = \frac{\mu}{a_\alpha a_\beta} \int_{v_\alpha} \int_{v_\beta} G(\mathbf{r}_\alpha, \mathbf{r}_\beta) dv_\alpha dv_\beta \quad (5a)$$

$$Pp_{ij} = \frac{1}{\varepsilon S_i S_j} \int_{S_i} \int_{S_j} G(\mathbf{r}_i, \mathbf{r}_j) dS_i dS_j \quad (5b)$$

Based on the electric field integral equation (EFIE), and a typical circuit model for a  $m$ -th cell is depicted in Fig. 3 [12]–[14]. In this figure,  $R_m$ ,  $Lp_{mm}$ ,  $Pp_{mm}$  and  $Pp_{m+1,m+1}$  are self resistance, inductance and self coefficients of potential for the circuit model, respectively. They correspond to  $\frac{\mathbf{J}}{\sigma}$ ,  $\frac{\partial \mathbf{A}}{\partial t}$  and  $\nabla \phi$  in (4), respectively.  $V_{m(i)}^C$  and  $V_{m(j)}^C$  are the voltage control voltage sources (VCVSs) due to mutual capacitive coupling between different capacitors.  $V_{m(k)}^L$  is the VCVS due to mutual coupling between  $Lp_{mm}$  and self inductors in other cells.

## III. AN EQUIVALENT CIRCUIT MODEL FOR ANISOTROPIC CONDUCTIVITY MEDIA

A surface discretization is applied to represent current and charge distributions on an infinitely thin graphene sheet. By considering the tensor effect of the surface conductivity, a new circuit model can be derived for the magnetized graphene.

Assume an infinitely thin graphene sheet is of the rectangular shape. Its surface discretization is shown in Fig. 4 [20]. The currents  $\mathbf{J}_X$  and  $\mathbf{J}_Y$ , are currents flowing on the graphene surface while the third current component  $\mathbf{J}_Z$  is zero.

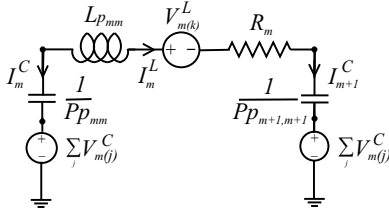


Fig. 3. One cell model for the  $m$ -th element, in which  $R_m$ ,  $Lp_{mm}$ ,  $Pp_{mm}$  and  $Pp_{m+1,m+1}$  are self resistance, inductance and self coefficients of potential for the circuit model, respectively. They correspond to  $\frac{1}{\sigma}$ ,  $\frac{\partial \mathbf{A}}{\partial t}$  and  $\nabla \phi$  in (4), respectively.  $V_{m(i)}^C$  and  $V_{m(j)}^C$  are the voltage control voltage sources (VCVSs) due to mutual capacitive coupling between different capacitors.  $V_{m(k)}^L$  is the VCVS due to mutual coupling between  $Lp_{mm}$  and self inductors in other cells.

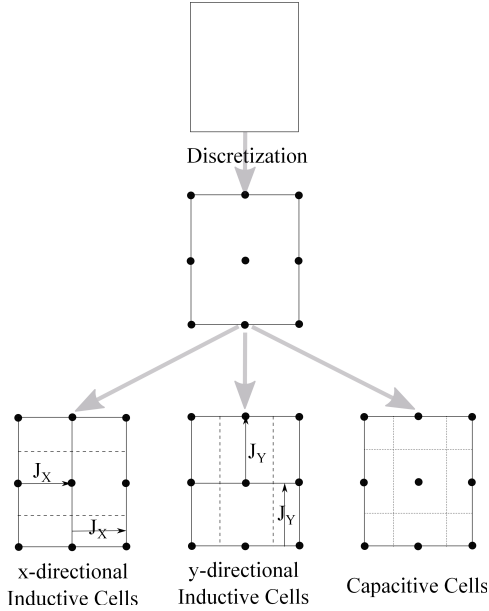


Fig. 4. 2D discretization of thin conductive plate. Dark circles indicate nodes, dashed lines separate inductive cells, and dotted lines separate capacitive cells.

According to the superposition of electric field on a conducting plate,

$$\begin{aligned} \mathbf{E}^{tot} &= \mathbf{E}^{inc} - \frac{\partial \mathbf{A}}{\partial t} - \nabla \phi \\ &= \bar{\bar{\sigma}}_g^{-1} \mathbf{J} \\ &= \bar{\bar{\rho}} \mathbf{J} \end{aligned} \quad (6)$$

where  $\mathbf{A}$  and  $\phi$  are vector and scalar potentials, respectively.  $\bar{\bar{\rho}}$  is the inverse of conductivity tensor  $\bar{\bar{\sigma}}_g$  and denotes resistivity of graphene. Hence the total electric field is represented by  $x$  and  $y$  components as follows

$$E_x^{tot} = \rho_{xx} J_x + \rho_{xy} J_y \quad (7a)$$

$$E_y^{tot} = \rho_{yx} J_x + \rho_{yy} J_y \quad (7b)$$

Combing Eq. (6) and Eq. (7), we have the starting equations for circuit model derivations.

$$\rho_{xx} J_x + \rho_{xy} J_y + \frac{\partial A_x}{\partial t} + \frac{\partial \phi}{\partial x} = -E_x^{inc} \quad (8a)$$

$$\rho_{yx} J_x + \rho_{yy} J_y + \frac{\partial A_y}{\partial t} + \frac{\partial \phi}{\partial y} = -E_y^{inc} \quad (8b)$$

#### A. $x$ -Directional Resistive Cell

According to (8a), the resistive contribution  $\rho_{yx} J_x$  in isotropic media is changed to  $\rho_{yx} J_x + \rho_{xy} J_y$ . It means that the resistive effect in one direction comes from contributions of two directions. Unlike isotropic materials, magnetically biased graphene couples the currents of orthogonal directions of two directions. In order to get the resistive components of graphene, we need to check the two terms carefully.

For a surface cell, the surface current densities in  $x$  and  $y$  directions are defined as  $J_x = I_x/l_y$ ,  $J_{iy} = I_{iy}/l_{ix}$ ,  $i = 1, 2, 3$  and 4.  $I_x$  is the current in  $x$ -directional inductive cell, and  $I_{iy}$  is the current of the  $i$ -th  $y$ -directional inductive cell.  $l_{ix}$  is the length of the  $i$ -th  $y$ -directional inductive cell. The areas of four small cells are all  $l_x/2 \times l_y/2$  in Fig. 5. Hence, the voltage drop caused by the resistive loss along the  $x$ -directional inductive cell is defined as

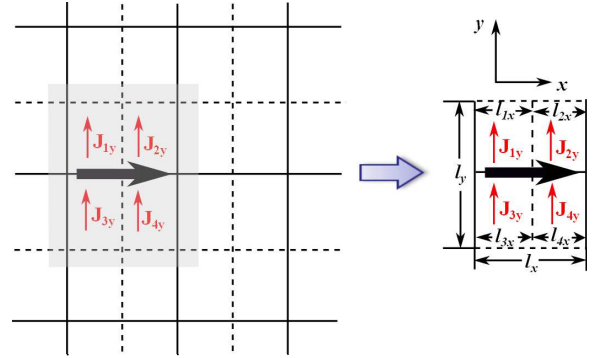


Fig. 5.  $x$ -directional graphene cell is studies first. The big black arrow shows  $x$ -directional current and red small arrows show  $y$ -directional currents.  $l_x$  and  $l_y$  denotes the length and width of the inductive cell, respectively. The studied inductive cell (in shadows) has constant  $x$ -directional current density  $J_x$  and this inductive cell is distributed into four nearby  $y$ -directional inductive cells whose current densities are  $J_{1y}$ ,  $J_{2y}$ ,  $J_{3y}$  and  $J_{4y}$ , respectively.  $l_{1x}$ ,  $l_{2x}$ ,  $l_{3x}$  and  $l_{4x}$  are the length of these current densities  $J_{1y}$ ,  $J_{2y}$ ,  $J_{3y}$  and  $J_{4y}$ , respectively.

$$V_R^x = R_x I_x + R_{1x} I_{1y} + R_{2x} I_{2y} + R_{3x} I_{3y} + R_{4x} I_{4y} \quad (9)$$

where

$$R_x = \rho_{xx} \frac{l_x}{l_y}, \quad (10a)$$

$$R_{ix} = \frac{\rho_{xy}}{l_{ix} l_y} \frac{l_x l_y}{2}, \quad i = 1, 2, 3, \text{ and } 4. \quad (10b)$$

$$I_{iy} = J_{iy} l_{ix}, \quad i = 1, 2, 3, \text{ and } 4. \quad (10c)$$

$R_{1x} - R_{4x}$  represent the coupled resistive effect from the  $y$ -direction current, and they are equivalent to the the coefficients of  $x$ -directional current control voltage sources (CCVSs).

According to (9), the resistive part of the equivalent circuit model can be illustrated as a resistor in series with four CCVSs (current control voltage sources), and is shown in Fig. 6. The remaining inductive and capacitive branches are the same with that of the non-magnetized graphene [4].

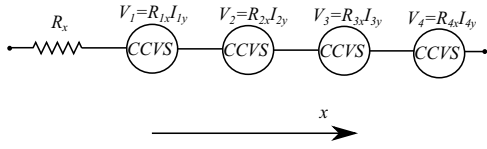


Fig. 6.  $x$ -directional resistive part of equivalent circuit model. The CCVSs are in series with a resistor.

### B. $y$ -Directional Resistive Cell

Similarly,  $y$ -directional circuit model for graphene can be derived using the mesh cell shown in Fig. 7. The currents are first defined as  $J_y = I_y/l_x$ ,  $J_{ix} = I_{ix}/l_{iy}$ ,  $i = 1, 2, 3$  and 4.  $I_y$  is the current in  $y$ -directional inductive cell, and  $I_{ix}$  is the current of the  $i$ -th  $x$ -directional inductive cell.  $l_{iy}$  is the length of the  $i$ -th  $x$ -directional inductive cell. The areas of four small cells are all  $l_x/2 \times l_y/2$  in Fig. 7. Hence, the voltage drop caused by the resistive loss along the  $y$ -directional inductive cell is defined as

$$V_R^y = R_y I_y + R_{1y} I_{1x} + R_{2y} I_{2x} + R_{3y} I_{3x} + R_{4y} I_{4x} \quad (11)$$

where

$$R_y = \rho_{yy} \frac{l_y}{l_x}, \quad (12a)$$

$$R_{iy} = \frac{\rho_{yx}}{l_{iy} l_x} \frac{l_x l_y}{2}, \quad i = 1, 2, 3, \text{ and } 4. \quad (12b)$$

$$I_{ix} = J_{ix} l_{iy}, \quad i = 1, 2, 3, \text{ and } 4. \quad (12c)$$

$R_{1y} - R_{4y}$  represent the coupled resistive effect from the  $y$  direction current, and they are equivalent to the coefficients of  $y$ -directional CCVSs.

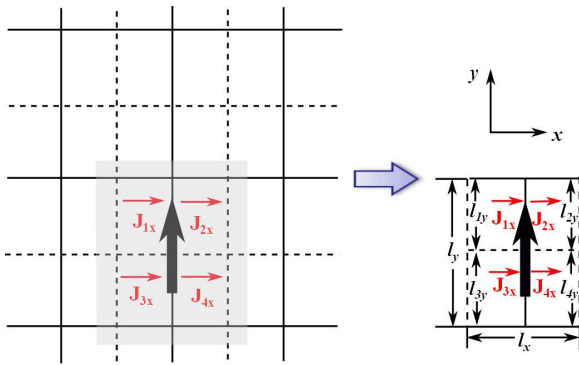


Fig. 7.  $y$ -directional graphene cell is studies first. The big black arrow shows  $y$ -directional current and red small arrows show  $x$ -directional currents.  $l_x$  and  $l_y$  denotes the length and width of the inductive cell, respectively. The studied inductive cell (in shadows) has constant  $y$ -directional current density  $J_y$  and this inductive cell is distributed into four nearby  $x$ -directional inductive cells whose current densities are  $J_{1x}$ ,  $J_{2x}$ ,  $J_{3x}$  and  $J_{4x}$ , respectively.  $l_{1y}$ ,  $l_{2y}$ ,  $l_{3y}$  and  $l_{4y}$  are the width of these current densities  $J_{1x}$ ,  $J_{2x}$ ,  $J_{3x}$  and  $J_{4x}$ , respectively.

According to (11), the resistive part of the equivalent circuit model can be illustrated as a resistor in series with four CCVSs (current control voltage sources), as shown in Fig. 8. The remaining inductive and capacitive branches are the same with that of the non-magnetized graphene [4].

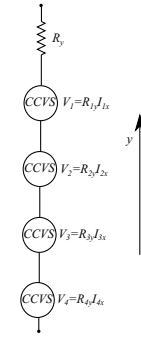


Fig. 8.  $y$ -directional resistive part of equivalent circuit model. The CCVSs are in series with a resistor.

### C. The Complete Equivalent Circuit for Biased Graphene

By combing the novel circuit model of  $x$ - and  $y$ -directional resistive part of resistance, the complete equivalent circuit suitable for anisotropic conductivity media is obtained. If four unit cells are placed along the  $x$  and  $y$  coordinates, the equivalent circuit for these nearby cells (two in  $x$ -direction and two in  $y$ -direction) is illustrated in Fig. 9.

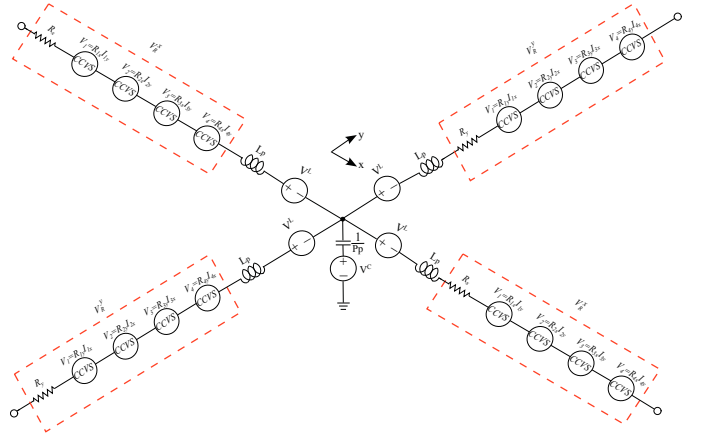


Fig. 9. A schematic diagram of the complete equivalent circuit for anisotropic conductivity graphene. This circuit model is for four nearby cells which share a common node. Two branches are for  $x$ -directional cells and the other two are for  $y$ -directional cells. The scripts for each cell are omitted for simplicity.

In Fig. 9, an equivalent circuit model for anisotropic graphene is sketched. The circuit elements inside the red rectangular dashed lines form the resistive part of  $x$  and  $y$ -directional voltage drop,  $V_R^x$  and  $V_R^y$ . This circuit model is for four nearby cells which share a common node, and two for  $x$ -directional cells and the other two for  $y$ -directional cells. In this figure, the scripts for each cell are omitted for simplicity, and all the elements in the model can be calculated according to the geometry and characteristics of each cell. This model is a combination of Fig. 6 and Fig. 8.

## IV. NUMERICAL EXAMPLES

### A. A Finite Size Graphene Patch

To validate the accuracy of the proposed algorithm for the magnetized graphene, a  $10$  by  $2 \mu\text{m}^2$  graphene patch is studied first. The graphene patch is biased by a  $z$ -directional

static magnetic field and is illuminated by a plane wave linearly polarized along the patch length, where  $\mathbf{k} = \hat{z}$  is the direction of propagation. Relaxation time  $t = 1.3 \times 10^{-13}$  s, the magnetostatic bias  $B_0 = 0.25$  T. The absorption cross section and extinction cross section calculated by this proposed equivalent circuit model and DG [21] (discontinuous Galerkin method) are compared in Fig. 10.

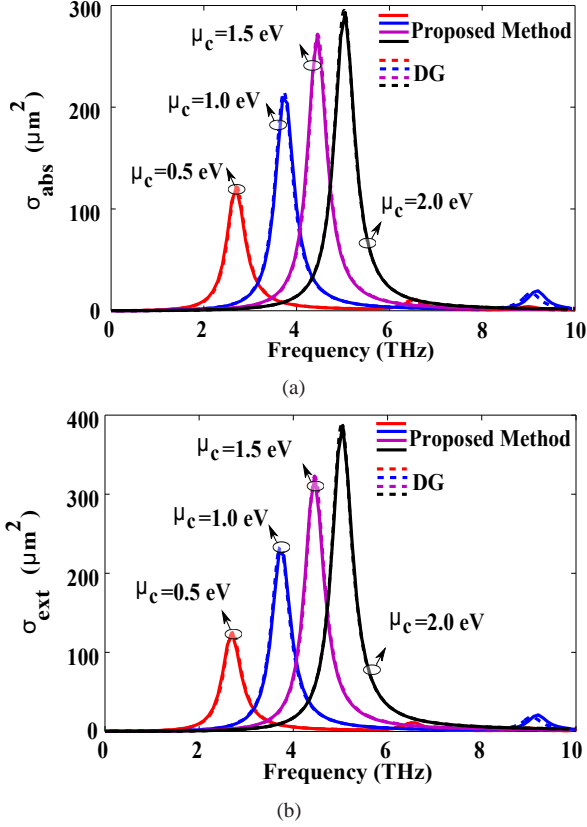


Fig. 10. The comparison of (a)  $\sigma_{abs}$  (absorption cross section), (b)  $\sigma_{ext}$  (extinction cross section) of the graphene patch calculated with the proposed equivalent circuit method and the discontinuous Galerkin method (DG).

From Fig. 10, it can be concluded that the absorption cross section and extinction cross section for the magnetized graphene patch calculated by this method match very well with the discontinuous Galerkin method, which validates the proposed method in this paper.

The normalized  $x$ -directional current distributions on the patch are also depicted in Fig. 11 for  $\mu_c = 1.0$  eV at the two resonant frequencies  $f_1 = 3.73$  THz and  $f_2 = 9.20$  THz. Since at the resonant frequencies, the current distributions behave like the near field electric field distribution, which illustrates that this model capture the physics very well.

## V. CONCLUSION

In this paper, a novel circuit method is proposed to characterize the statically magnetized biased graphene. In order to better analyze its anisotropic and dispersive properties, a new equivalent circuit with CCVSs is developed to incorporate the off-diagonal elements of the conductivity tensor. Several examples are presented to verify this method and to illustrate

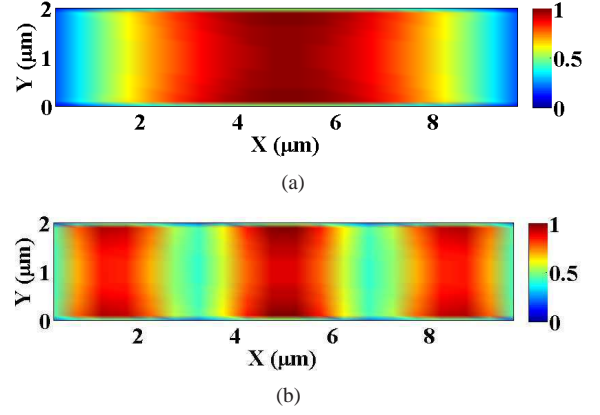


Fig. 11. The comparison of normalized  $x$ -directional current distributions at the two resonant frequencies (a)  $f_1 = 3.73$  THz, (b)  $f_2 = 9.20$  THz.

the physical meanings of the CCVSs. This is the first equivalent circuit-based approach to deal with anisotropic graphene according to the authors' knowledge.

## ACKNOWLEDGMENT

This work was supported in part by the Research Grants Council of Hong Kong (GRF 712612 and 711511), NSFC 61271158, HKU Seed Fund 201309160052, and Hong Kong UGC AoE/P-04/08. The authors are also grateful for the helpful comments from reviewers, editors, and for the constructive suggestions from Prof. W. C. Chew.

## APPENDIX A THE CONDUCTIVITY TENSOR

### A. Rigorous Formula of the Surface Conductivity Tensor

By counting both intraband and interband contributions of graphene, the rigorous explicit expressions of  $\sigma_d$  and  $\sigma_o$  in (3) are [18]

$$\begin{aligned} & \sigma_d(\mu_c(E_0), B_0) \\ &= \frac{e^2 v_F^2 |eB_0| (\omega - j2\Gamma)\hbar}{-j\pi} \\ & \times \sum_{n=0}^{\infty} \left\{ \frac{f_d(M_n) - f_d(M_{n+1}) + f_d(-M_{n+1}) - f_d(-M_n)}{(M_{n+1} - M_n)^2 - (\omega - j2\Gamma)^2 \hbar^2} \right. \\ & \times \left( 1 - \frac{\Delta^2}{M_n M_{n+1}} \right) \frac{1}{M_{n+1} - M_n} \\ & + \frac{f_d(-M_n) - f_d(M_{n+1}) + f_d(-M_{n+1}) - f_d(-M_n)}{(M_{n+1} - M_n)^2 - (\omega - j2\Gamma)^2 \hbar^2} \\ & \left. \times \left( 1 + \frac{\Delta^2}{M_n M_{n+1}} \right) \frac{1}{M_{n+1} + M_n} \right\} \end{aligned} \quad (13)$$

and

$$\begin{aligned} & \sigma_o(\mu_c(E_0), B_0) \\ &= -\frac{e^2 v_F^2 |eB_0|}{\pi} \\ & \sum_{n=0}^{\infty} \{f_d(M_n) - f_d(M_{n+1}) + f_d(-M_{n+1}) - f_d(-M_n)\} \\ & \times \left\{ \left(1 - \frac{\Delta^2}{M_n M_{n+1}}\right) \frac{1}{(M_{n+1} - M_n)^2 - (\omega - j2\Gamma)^2 \hbar^2} \right. \\ & \left. \times \left(1 + \frac{\Delta^2}{M_n M_{n+1}}\right) \frac{1}{(M_{n+1} - M_n)^2 - (\omega - j2\Gamma)^2 \hbar^2} \right\} \end{aligned} \quad (14)$$

where

$$M_n = \sqrt{\Delta^2 + 2n v_F^2 |eB_0| \hbar} \quad (15)$$

and  $-e$  is the charge of an electron,  $\hbar$  is the reduced Planck's constant,  $B_0$  is the static magnetic field, and  $f_d$  is the Fermi-Dirac distribution. And

$$f_d(\varepsilon) = (e^{(\varepsilon - \mu_c)/k_B T} + 1)^{-1} \quad (16)$$

where  $\varepsilon$  is energy, and  $k_B$  is the Boltzmann's constant.

### B. Intraband Approximation

The analytical expressions for surface conductivity  $\sigma_d$  and  $\sigma_o$  are composed of intraband and interband contributions. The rigorous explicit expressions of  $\sigma_d$  and  $\sigma_o$  in (3) are [18]. For frequencies within THz band, the intraband term is dominant in the total conductivity. For simplicity, the expressions of  $\sigma_d$  and  $\sigma_o$  can be approximated by a Drude-like model [6], [19], which are

$$\sigma_d = \sigma \frac{1 + j\omega t}{(\omega_c t)^2 + (1 + j\omega t)^2} \quad (17a)$$

$$\sigma_o = \sigma \frac{\omega_c t}{(\omega_c t)^2 + (1 + j\omega t)^2} \quad (17b)$$

with

$$\sigma = \frac{e^2 t k_B T}{\pi \hbar^2} \left[ \frac{\mu_c}{k_B T} + 2 \ln(e^{-\mu_c/k_B T} + 1) \right] \quad (18)$$

where  $T$  is the Kelvin temperature,  $t$  is the relaxation time, and  $\omega_c$  is the cyclotron frequency with  $\omega_c = eB_0 v_F^2 / \mu_c$  and  $v_F = 10^6$  m/s denotes the Fermi velocity.

## APPENDIX B

### EXTINCTION, ABSORPTION AND SCATTERING CROSS SECTIONS

The extinction power is the total power removed from the incident field (the sum of the absorbed and the scattered powers) due to the presence of the scattering object  $\Omega$ . The absorbed power is the power flowing into the body and the power scattered from an object  $\Omega$  is given by the real part of the integral of the outward-directed normal component of  $\mathbf{S}_{sca}$  over  $\partial\Omega$ .  $\mathbf{S}_{tot}$  is the time average Poynting vector.  $\mathbf{S}_{inc}$ ,  $\mathbf{S}_{sca}$

and  $\mathbf{S}_{ext}$  are incident, scattered and extinguished components of the Poynting vector. According to [16],  $P_{ext} = P_{sca} + P_{abs}$ .

$$P_{abs} = \oint_{\partial\Omega} \langle \mathbf{S}_{tot} \rangle \cdot \hat{\mathbf{n}} \quad (19a)$$

$$P_{sca} = \oint_{\partial\Omega} \langle \mathbf{S}_{sca} \rangle \cdot \hat{\mathbf{n}}. \quad (19b)$$

According to the distributed power characterization [11], the absorbed and scattered power can be represented by the current distributions and the partial elements, which are

$$P_{abs} = P^{ohm} \quad (20a)$$

$$P_{sca} = P^r \quad (20b)$$

where  $P^r$  and  $P^{ohm}$  are the radiated power and ohmic power loss. They can be conveniently represented and calculated based on the new method in [11], without involving field calculation and far field integration. For instance, the radiated and ohmic power from the segmentation  $a$  is formulated as:

$$P_{a(a)}^{r'} = \frac{1}{2} \text{Re}(\mathbf{I}_a^{L\dagger} \bar{\mathbf{Z}}_L^{aa} \mathbf{I}_a^L + \mathbf{I}_a^{C\dagger} \bar{\mathbf{Z}}_C^{aa} \mathbf{I}_a^C). \quad (21a)$$

$$P_a^{ohm} = \frac{1}{2} \mathbf{I}_a^{L\dagger} \bar{\mathbf{Z}}_{ohm}^{aa} \mathbf{I}_a^L \quad (21b)$$

where the superscript ' $\dagger$ ' means the conjugate transpose of a vector.  $\mathbf{I}_a^L$  is the vector of current distribution of inductive branches on  $a$ .  $\bar{\mathbf{Z}}_L^{aa}$  is an  $N_{L_a} \times N_{L_a}$  matrix in which all elements are inductive coupling impedances ( $N_{L_a}$  and is the number of inductive cells on  $a$ .  $\bar{\mathbf{Z}}_{L(mk)}^{aa} = j\omega L p_{mk}$ ),  $\bar{\mathbf{Z}}_C^{aa}$  is an  $N_{C_a} \times N_{C_a}$  matrix whose elements correspond to capacitive coupling ( $N_{C_a}$  is the number of capacitive cells on  $a$ .  $\bar{\mathbf{Z}}_{C(mk)}^{aa} = \frac{p_{mk}}{j\omega}$ ).  $\bar{\mathbf{Z}}_{ohm}^{aa}$  is a diagonal matrix which contains the resistive part of each cell.

Based on the power analysis [11], the absorption, scattering and extinction cross section are reformulated as

$$\sigma_{abs} = \frac{P_{abs}}{|\mathbf{S}_{inc}|}. \quad (22a)$$

$$\sigma_{sca} = \frac{P_{sca}}{|\mathbf{S}_{inc}|}. \quad (22b)$$

$$\sigma_{ext} = \sigma_{abs} + \sigma_{sca}. \quad (22c)$$

Equation (21) - (22) convert the calculation process for cross sections into an intrinsic circuit problem that can be solved without involving direct electric and magnetic field calculations.

## REFERENCES

- [1] F. Schwierz, "Graphene transistors," *Nature Nanotech.*, vol. 5, pp. 487–496, May 2010.
- [2] M. Tamagnone, J. S. Gomez-Diaz, J. R. Mosig, and J. P. Carrier, "Analysis and design of terahertz antennas based on plasmonic resonant graphene sheets," *Appl. Phys. Lett.*, vol. 101, no. 214102, pp. 1–4, 2012.
- [3] F. H. L. Koppens, D. E. Chang, and F. J. G. Abajo, "Graphene plasmonics: a platform for strong light–matter interactions," *Nano Lett.*, vol. 11, pp. 3370–3377, Jul. 2011.
- [4] Ying S. Cao, Li Jun Jiang, A. E. Ruehli, "An equivalent circuit model for graphene-based terahertz antenna using the PEEC method," submitted.
- [5] O. V. Shapoval, J. S. G-Diaz, J. P-Carrier, J. R. Mosig, and A. I. Nosich, "Integral equation analysis of plane wave scattering by coplanar graphenestrip gratings in the THz range," *IEEE Trans. Terahertz Sci. Techn.*, vol. 6, no. 3, pp. 666–674, Sept. 2013.
- [6] V. Nayyeri, M. Soleimani, and M. Ramahi, "Wideband modeling of graphene using the finite-difference time-domain method," *IEEE Trans. Antennas Propag.*, vol. 6, no. 12, pp. 6107–6114, Dec. 2013.
- [7] Y. S. Cao, L. J. Jiang and A. E. Ruehli, "An Equivalent Circuit Model for Graphene-based Terahertz Antenna Using the PEEC Method," submitted to *IEEE Trans. Antennas Propag.*.
- [8] N. Chamanara, D. Sounas, and C. Caloz, "Non-reciprocal magnetoplasmon graphene coupler," *Opt. Express*, vol. 21, no. 9, pp. 11248–11256, May 2013.
- [9] G. W. Hanson, "Dyadic Green's functions for an anisotropic, non-local model of biased graphene," *IEEE Trans. Antennas Propag.*, vol. 56, no. 3, pp. 747–757, Mar. 2008.
- [10] X. H. Wang, W. Y. Yin, and Z. Chen, "Matrix exponential FDTD modeling of magnetized graphene sheet," *IEEE Antennas Wireless Propag. Lett.*, vol. 12, pp. 1129–1132, Dec. 2013.
- [11] Ying S. Cao, Li Jun Jiang and A. E. Ruehli, "Distributive radiation and transfer characterization based on the PEEC method," *IEEE Trans. Electromag. Compat.*, vol. 57, no. 4, Aug. 2015.
- [12] A. E. Ruehli, "Equivalent circuit models for three dimensional multi-conductor systems," *IEEE Trans. Microw. Theory Tech.*, vol. MTT-22, no. 3, pp. 216–221, Mar. 1974.
- [13] A. E. Ruehli, "Inductance calculations in a complex integrated circuit environment," *IBM J. Res. Develop.*, vol. 16, no. 5, pp. 470–481, Sep. 1972.
- [14] A. E. Ruehli and P. A. Brennan, "Efficient capacitance calculations for three-dimensional multiconductor systems," *IEEE Trans. Microw. Theory Tech.*, vol. 21, no. 2, pp. 76–82, Feb. 1973.
- [15] G. Lovat, "Equivalent circuit for electromagnetic interaction and transmission through graphene sheets," *IEEE Trans. Electromagn. Compat.*, vol. 54, no. 1, pp. 101–109, Feb. 2012.
- [16] C. F. Bohren and D. R. Huffman, *Absorption and Scattering of Light by Small Particles*, Wiley Interscience: New York, 1983.
- [17] G. W. Hanson, "Dyadic Green's functions for an anisotropic, non-local model of biased graphene," *IEEE Trans. Antennas Propag.*, vol. 56, no. 3, pp. 747–757, Mar. 2008.
- [18] V. P. Gusynin, S. G. Sharapov, and J. P. Carbotte, "Magneto-optical conductivity in graphene," *J. Phy. Condens. Matter*, vol. 19, p. 026222 (1–25), 2007.
- [19] D. L. Sounas and C. Caloz, "Gyrotropy and nonreciprocity of graphene for microwave applications," *IEEE Trans. Microw. Theory Tech.*, vol. 60, no. 4, pp. 901–914, Apr. 2012.
- [20] J. Ekman, "Electromagnetic modeling using the Partial Element Equivalent Circuit method," Ph.D. dissertation, Lulea University of Technology, Sweden, 2003.
- [21] P. Li, and L. J. Jiang, "Modeling of magnetized graphene from microwave to THz range by DGTD with a scalar RBC and an ADE ", *IEEE Trans. Antennas Propag.*, vol. 63, no. 10, Oct. 2015.